Optical control of Faraday rotation in hot Rb vapor

Paul Siddons, Charles S. Adams, and Ifan G. Hughes
Department of Physics, Durham University, South Road, Durham DH1 3LE, United Kingdom
(Received 8 December 2009; revised manuscript received 16 March 2010; published 27 April 2010)

We demonstrate controlled polarization rotation of an optical field conditional on the presence of a second field. Induced rotations of greater than $\pi/2$ rad are seen with a transmission of 95%, corresponding to a ratio of phase shift to absorption of 40π. This combination of large, controlled rotation and low loss is well suited for the manipulation of light pulses.

DOI: 10.1103/PhysRevA.81.043838 PACS number(s): 42.70.Nq, 33.57.+c

I. INTRODUCTION

The ability to manipulate optical pulses is central to the advancement of information and communications technology [1]. All-optical switching [2] has the advantage that the optical information can be processed without conversion to an electrical signal. An all-optical switch is produced by using an optical control field to modify the refractive index or the absorption of the medium, that is, the real or the imaginary part of the electrical susceptibility, χ^R or χ^I. For example, in electromagnetically induced transparency (EIT) [3,4] or off-resonance Raman resonances [5–7], a strong control field is employed to reduce the absorption at a particular frequency. Reduction of the intensity of the control field to the single-photon level is of interest for certain quantum information protocols [8]. All-optical switching at low light levels has been demonstrated using EIT [9] and also using transverse optical pattern formation [10,11].

An additional important criterion in an optical switch is high-fidelity transmission of the input field to reduce the loss of information. The requirement of a large modulation depth concomitant with low absorption suggests that control of the phase, or χ^R, is preferable, as in electro-optic devices such as the Mach-Zehnder modulator [12]. In this case, the figure of merit of the switching process is characterized by the change in the birefringence of the medium divided by absorption, $\Delta\chi^R/\chi^I$, that is, the ratio of the phase shift to the optical depth d, $2\Delta\phi/d$. We note that, for a two-state resonance, the Kramers-Kronig relations show that this ratio is largest far from resonance, where the dispersion is also smaller [13]. The change in χ^R can be between different polarization modes of the light field, giving rise to birefringence or Faraday rotation. Polarization rotation of a linearly polarized optical field has been studied extensively in atomic systems. Such rotations may be induced by an applied magnetic field, the Faraday effect [14–16], by an applied electric field [17], or by spin-polarizing the medium, the paramagnetic Faraday effect [18–22]. For optical switching, a rotation angle of $\pi/2$ rad is required such that two orthogonal linear polarization modes can be exchanged. An EIT scheme reported by Li *et al.* provides rotations in the region of $\pi/4$ rad, with ~50% loss [23]. Larger rotations at lower loss were seen by Siddons *et al.* using the off-resonant Faraday effect [16], but without optical control.

In this paper we demonstrate high-fidelity modulation (>90%) of the input field using optical control in an atomic vapor. To achieve a large induced rotation with low loss, that is, a high value of the figure of merit $\Delta\chi^R/\chi^I$, we bias the rotation of the probe using the off-resonant Faraday effect and employ a control beam to induce population transfer to modulate around this bias. We demonstrate optical control of the Faraday rotation owing both to changes in the total number of atoms and to their spin distribution. For a probe field detuned by more than five times the inhomogeneous atomic linewidth, we observe a phase shift of $\pi/2$ rad with a loss below 5%, corresponding to $\Delta\chi^R/\chi^I = 40\pi$. This combination of large dispersion and low loss is interesting in the context of all-optical manipulation of light pulses. Since a large rotation is achieved off resonance, the process potentially can be operated at high bandwidth of the order of gigahertz [16]. In addition, by combining this technique with the dispersive filtering properties of the Faraday effect [15,24,25], one could realize an optically tunable narrowband filter.

The structure of this paper is as follows. In Secs. II and III we present the theory behind the Faraday effect and relate it to measurable quantities. In Sec. IV we describe the experimental apparatus, giving the results of our investigation in Secs. V and VI, before drawing our conclusions in Sec. VII.

II. BIREFRINGENCE IN AN ATOMIC MEDIUM

In an atomic medium left- (right-)circularly polarized light stimulates σ^+ (σ^-) optical transitions when the axis of quantization is taken to be in the direction of light propagation [Fig. 1(i)]. The effect of a magnetic field applied along the quantization axis is to shift the energy levels such that, for a particular frequency of light, the σ transitions are shifted from resonance. If one of the σ transitions is closer to resonance than the other, the strengths are unequal. This is illustrated in Fig. 1(ii). For incident linearly polarized light (equal amounts of left- and right-circular polarizations), an asymmetry in the refractive indices of the σ transitions results in a rotation of the plane of polarization: the Faraday effect.

Any method of altering the birefringence of a medium can result in polarization rotation. One example is illustrated in Fig. 1(iii). Here, instead of a magnetic field being used to break the degeneracy of the system and thereby introduce birefringence into the medium, the populations of the transition ground states are altered, which causes birefringence by changing the relative strengths of the σ transitions. The redistribution of angular momentum states gives a net spin polarization to the medium; hence the name "paramagnetic

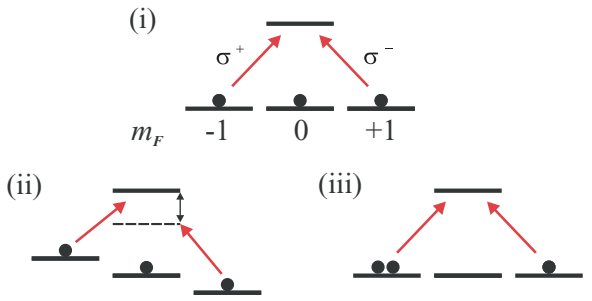

FIG. 1. (Color online) An illustration of energy-level configurations leading to circular birefringence. (i) The energies of the σ transitions are degenerate, and the states are equally populated: no asymmetry is seen for circularly polarized light. (ii) An applied magnetic field lifts the degeneracy to such an extent that, while the σ^+ transition is resonant, the σ^- is detuned further from resonance. (iii) While both transitions are resonant, a population difference is present, leading to birefringence.

Faraday effect," although strictly it is unrelated to the magneto-optic Faraday effect since an applied magnetic field is not required. The spin polarization is typically achieved via optical pumping on a σ transition to an auxiliary excited state, so the probe polarization is controlled by the pumping field.

To our knowledge rotations of $\pi/2$ rad have not been demonstrated using optically induced birefringence (the paramagnetic Faraday effect). As rotations of $\pi/2$ rad are easily produced using magnetically induced birefringence (the Faraday effect), optical control can be introduced by using population transfer to modify the magnetically induced rotation. Here the static applied magnetic field produces a rotation offset to the probe beam, around which the polarization angle can be tuned via the optical control field.

III. MEASUREMENT OF THE POLARIZATION ROTATION

We measure the angular rotation θ of the polarization plane of probe light using a balanced polarimeter. We set a polarization beam splitter at $\pi/4$ rad to the linearly polarized probe such that the signal is zero in the absence of any optical rotation, as the light intensities of the horizontal, I_x, and vertical, I_y, channels of light incident on the detector are equal [26]. For an input polarization $\mathbf{e} = (\hat{\mathbf{x}} + \hat{\mathbf{y}})/\sqrt{2}$, the output intensity signals for an initial intensity $I_0 = I_{x_0} + I_{y_0}$ are [16]

$$(I_x - I_y)/I_0 = \sin(2\theta)\mathrm{e}^{-(\alpha^+ + \alpha^-)L/2}, \quad (1)$$

$$(I_x + I_y)/I_0 = \tfrac{1}{2}(\mathrm{e}^{-\alpha^+ L} + \mathrm{e}^{-\alpha^- L}), \quad (2)$$

where L is the length of the medium, and $\alpha^\pm$ are the absorption coefficients of the $\sigma^\pm$ transitions. The magnetically induced birefringence responsible for polarization rotation thus also causes circular dichroism (polarization-dependent absorption), both effects being strongest close to resonance. Hence at large detunings the incident light retains its linear polarization while being rotated; near-resonant light experiences greater rotation at the expense of becoming highly elliptical. The differencing signal [Eq. (1)] is a sinusoidal function delineated by the transmission caused by the average absorption coefficient, while the total intensity signal [Eq. (2)] is the average transmission of the two circular polarizations. In typical polarimetry experiments, a measurement of the rotation angle is achieved by normalization of the difference in the two channels by the sum. For cases of low absorption ($\alpha^\pm L \ll 1$) or negligible circular dichroism ($\alpha^+ \approx \alpha^-$), the ratio of Eqs. (1) and (2) reduces to $\sin(2\theta)$. However, these conditions are not met close to resonance. A rotation measurement that is independent of dichroism can be made by recording an additional differencing signal, this time with a half-wave plate before the analyzing cube [23]. This changes the sine dependence in Eq. (1) to a cosine dependence. Both signals are derived from a single beam that has propagated through the medium; hence the ratio of the two differencing signals is independent of absorption. While such a measurement is acceptable for small angles, it is discontinuous at rotations of $\pm\pi/4$ to the incident beam. Under typical experimental conditions the spectra we observe exhibit rotations of greater magnitude than these limits.

Given these considerations, we choose to present the differencing signal, as it conveys both the birefringent and dichroic characteristics of the medium. The rotation angle is extracted from this signal by looking at the zero crossings and extrema. Figure 2(i) shows a typical differencing signal in rubidium vapor [13,16] (the measurement of which is described in Sec. IV) and the calculated theoretical signal obtained by diagonalizing the complete Hamiltonian of the system. Good agreement with experimental data is seen: any discrepancy is due to the different detectors used in the measurement of I_x and I_y. For the differencing signal, as the probe detuning is increased, $\theta \to 0$, and thus the signal tends to zero. As the light nears resonance, the rotation increases from zero, and, because of the signal's sinusoidal dependence on θ, oscillations are observed. As can be seen by comparison

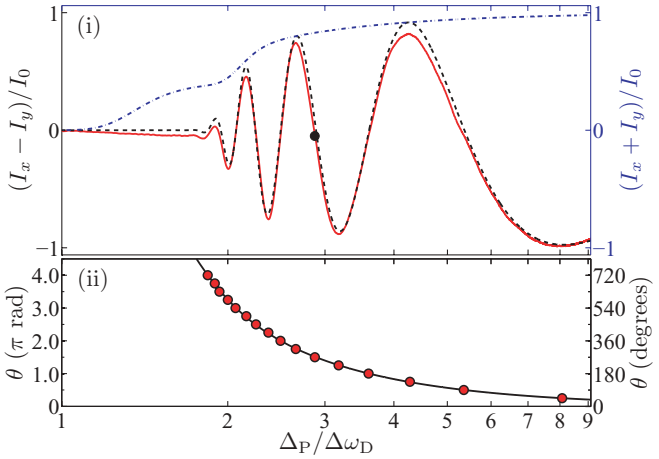

FIG. 2. (Color online) (i) Probe signal produced by scanning the probe versus red detuning Δ_P, from the D_1 ^{87}Rb $F = 2 \to F' = 1$ transition in units of Doppler width $\Delta\omega_D = 2\pi \times 571$ MHz. The red and dashed black curves show, respectively, the measured and theoretical differencing signal (left axis). The dot-dashed blue curve shows the total transmission through the cell (right axis). (ii) The measured rotation angle (data points) and theoretical rotation (curve). The temperature of the cell is 115°C and the applied magnetic field is 204 G.

of Figs. 2(i) and 2(ii), zero crossings correspond to rotations of integer multiples of $\pi/2$ rad to the incident beam; extrema correspond to $\pm\pi/4$ rad.

The total intensity signal is related to the dichroism of the medium, shown in Fig. 2. It is unity far from resonance, where there is little absorption, and zero on resonance because of the large optical depth at the parameters for which the signal is calculated. At detunings of greater than two Doppler widths, the peaks of the differencing signal lie close to the total intensity signal. At detunings closer to resonance, circular dichroism becomes important, with the knee indicating where one circular polarization is absorbed significantly more than the other. The light polarization here is almost circular; hence the differencing signal is zero.

IV. EXPERIMENTAL METHOD

Figure 3 shows a schematic of the experimental apparatus along with the energy-level scheme used to observe the optically controlled Faraday effect on the D_1 ($5^2S_{1/2} \rightarrow 5^2P_{1/2}$) transition of rubidium. The source of probe light was an external cavity diode laser at 795 nm. The probe-laser output polarization was linearly polarized and attenuated to be less than 1 μW. The beam had a $1/e^2$ radius of 0.8 mm. After passing through a half-wave plate, the beam was sent through a 75-mm heated vapor cell containing the Rb isotopes according to the ratio ^{87}Rb:^{85}Rb of 99:1. Heating and magnetic field were provided by a solenoid, based on the design of Ref. [27]. Upon transmission through the cell, the two orthogonal linear polarizations of the beam were separated with a polarizing beam splitter cube and sent to a differencing photodiode.

To observe the Faraday effect, only the probe beam and the applied magnetic field need be present (as in Fig. 2). To investigate optical control of the Faraday rotation, we added a counterpropagating control field resonant with the D_2 line ($5^2S_{1/2} \rightarrow 5^2P_{3/2}$) at 780 nm. The control beam was linearly polarized with a spot size of 2 mm ($1/e^2$ radius) and had a crossing angle of ~5 mrad with respect to the probe beam. A

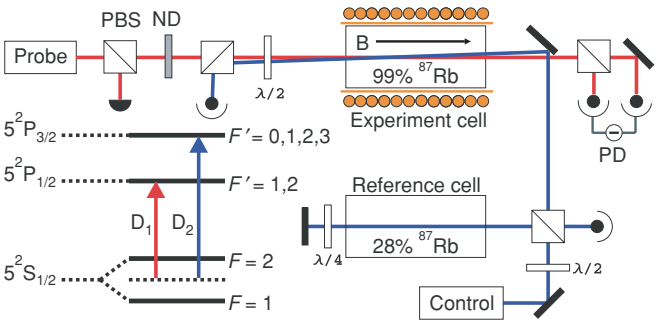

FIG. 3. (Color online) Schematic of the experimental apparatus. A probe beam passes through a polarization beam splitter (PBS), providing linearly polarized light. The beam is attenuated with a neutral-density filter (ND) before passing through a heated vapor cell. A half-wave plate ($\lambda/2$) is used to control the polarization angle of the light before it is analyzed with a PBS and collected on a differencing photodiode (PD). A control beam is linearly polarized and counterpropagated at a small crossing angle. A small fraction of the beam is used to perform sub-Doppler spectroscopy in a reference cell.

natural-abundance Rb cell was used as a frequency reference to calibrate the detuning of the control field relative to the D_2 line (see Fig. 3).

V. SPECTRAL DEPENDENCE OF FARADAY ROTATION ON THE OPTICAL CONTROL FIELD

To investigate optical control of Faraday rotation, we first look at the effect of scanning the control field close to resonance. We fix the detuning of the probe laser at a frequency where the polarimeter signal is close to zero (indicated by the dot in Fig. 2). Hence, any effect caused by the control field will be seen in the measurement of the probe differencing signal as a deviation from zero. In Fig. 4 we show the response of the Faraday rotation signal as a function of the detuning of the control field, Δ_C. Figure 4(i) shows the probe differencing signal for the same temperature and magnetic field as in Fig. 2. Figure 4(ii) shows the transmission of the control beam through the experiment cell and of a weaker beam through the reference cell. Between the two ^{87}Rb absorption lines, the control field appears to have little effect on the difference signal, but close to resonance and at greater detunings the effect of optical control is significant. The maximum (minimum) signal corresponds to alignment with the x (y) axis before it folds back upon itself at greater rotation angles. Increase in the control power increases the rotation angle while retaining similar spectral dependence; hence the dips seen in the 30 mW curve in Fig. 4(i) correspond to rotations beyond $\pi/4$ rad to the input beam, most noticeable at points A and B.

As previously mentioned, we chose to show the differencing signal to convey the absorptive as well as the dispersive effect on the probe beam. Since the presence of the control alters the dichroism experienced by the probe in a way that is

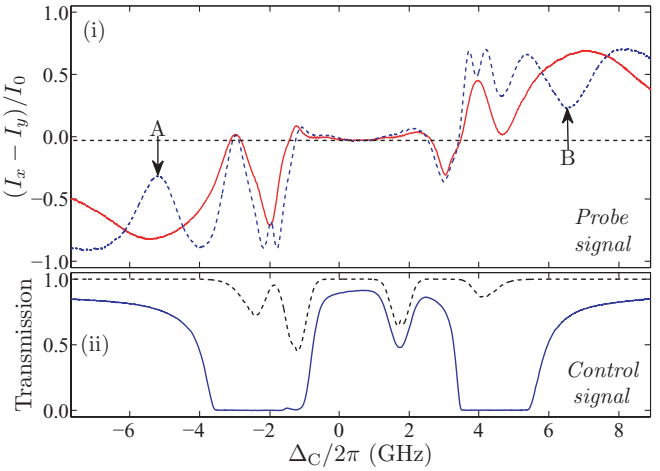

FIG. 4. (Color online) (i) Differencing signal of the D_1 probe versus D_2 control field blue detuning Δ_C. The power of the control field is 9 (solid red) and 30 mW (dashed blue). The experiment cell is at a temperature of ~115 °C, with a 204 G applied magnetic field. The probe is at a red detuning of ~2.9 Doppler widths (1.7 GHz), marked in Fig. 2. In the absence of the control field, the differencing signal is given by the horizontal dashed black line. (ii) Transmission of the control-laser light through the room-temperature natural-abundance reference cell (dashed black) and the ^{87}Rb experiment cell (blue). Control detuning is with respect to the weighted D_2 line center.

spectrally dependent, calculation of the rotation by division by the total intensity signal (as described in Sec. III) will give a false impression of the angle so obtained. For example, the magnitudes of the maximum (∼0.7) and minimum (∼0.9) signals in Fig. 4(i) are not equal because the control beam has increased the dichroism of the medium for positive detunings and decreased it for negative detunings. More reliable measurements of rotation are presented in the next section.

VI. OPTICAL CONTROL OF THE PROBE DIFFERENCING SIGNAL

In Sec. V we observed that the largest change to the birefringence of the medium was at control detunings either side of the D_2 transition. We now wish to find the spectral dependence of birefringence for the probe beam by scanning its frequency in a region red-detuned from the D_1 line. Figure 5 shows the resulting difference signal produced in the presence of the D_2 control field. Figures 5(i) and 5(ii) show the influence of the applied control field with its frequency fixed at the two points of maximum rotation shown in Fig. 4. From these plots we are able to obtain the absolute angular rotation θ of the probe using the zero crossings and extrema (which are independent of absorption or dichroism). The measured rotations are shown in Fig. 6. It can be seen that rotations of many π rad are possible with the Faraday effect, as observed in previous studies [13,16]. For the rotation angle of $\pi/2$ rad induced by the applied magnetic and optical fields, the change in refractive index $\Delta n = 5 \times 10^{-6}$, although changes of 10^{-4} and higher are possible for larger fields (see Ref. [16]).

To calculate the optically induced rotations, we extended our steady-state model used to generate the theory curve in Fig. 2 by setting the populations of the atomic states as independent parameters. This model quantitatively imitates the behavior of the optical pumping inducing the controlled Faraday rotation. Population transfer via a π-polarized pump is modeled as a change in the F-state populations; transfer

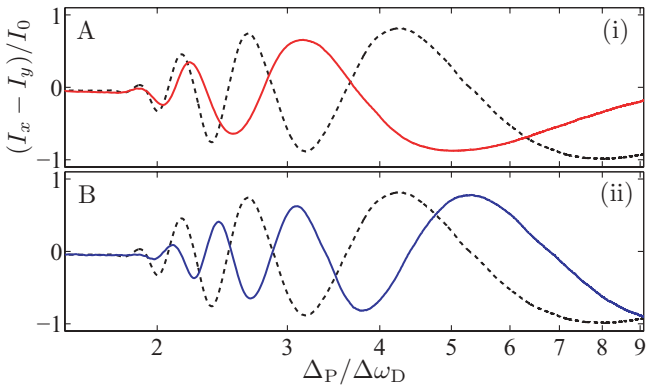

FIG. 5. (Color online) Differencing signal of the D_1 probe versus red detuning Δ_P. The dashed black curve shows the experimentally measured signal in the absence of the D_2 control field (from Fig. 2). Plots (i) and (ii) illustrate the effect of optical pumping on the probe signal when the 38-mW control field is fixed at detunings A and B given in Fig. 4. The temperature and applied magnetic field are the same as in Fig. 2.

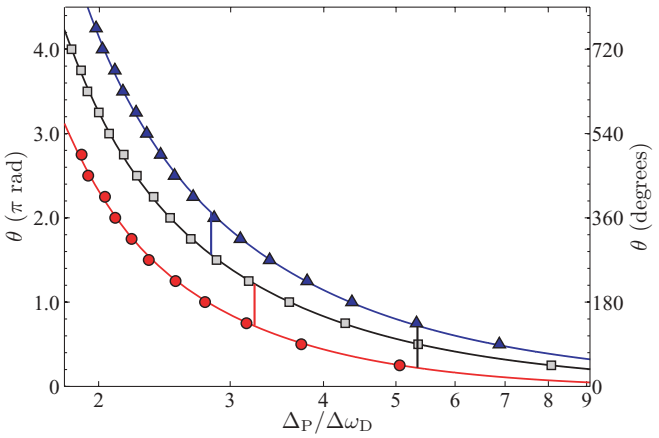

FIG. 6. (Color online) Measured rotation angles θ versus red detuning Δ_P of the D_1 probe. The angles are calculated from the zero crossings and extrema of Fig. 5 for no optical control (squares) and red-detuned (circles) and blue-detuned (triangles) control fields. The curves are from theory. Vertical bars show the detunings at which $\pi/2$ rotations can be obtained by switching among the three curves.

by $\sigma^{\pm}$ pumping is modeled as an anisotropy in the m_F-state populations: the paramagnetic Faraday effect. For the case of no pumping, an equilibrium population produces an excellent fit to data. Decrease in the population of the ^{87}Rb $F = 2$ state by 2.5%, with an m_F anisotropy such that there is an increased occupation of the $m_F = -2, -1$ states, reproduces the effect of a red-detuned control field; increase in the population by

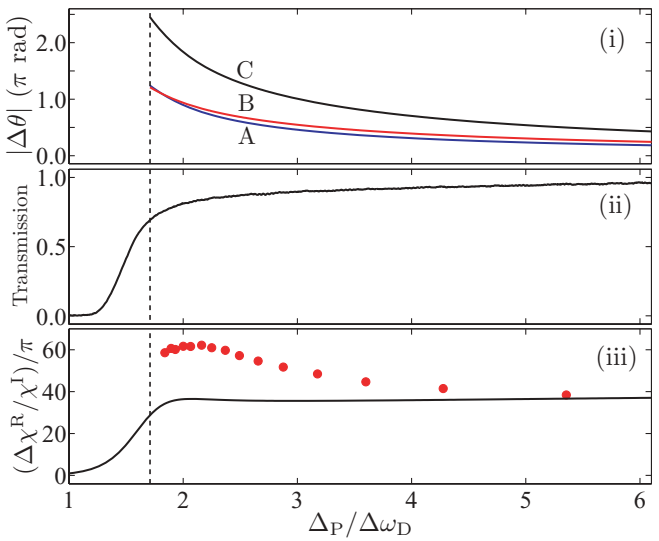

FIG. 7. (Color online) (i) Rotation difference between the cases with and without the optical control field, obtained from the experimental data shown in Fig. 6. Curves A (blue) and B(red) are, respectively, for blue and red detunings. Curve C (black) shows the rotation difference between blue and red detunings. (ii) Measured transmission of the linear probe in zero magnetic field. (iii) Figure of merit of the switching scheme: The curve was obtained from theory; the points show measured data. The dashed vertical line marks the limit close to resonance where the probe polarization becomes elliptical owing to circular dichroism (differential absorption of the left- and right-circularly polarized field components).

16%, with an m_F anisotropy that increases the occupation of the $m_F = 2,1$ states, reproduces the blue-detuned control field effect. The parameters used here on an *ad hoc* basis agree with the expected pumping behavior: the red-detuned beam pumps depletes the population of the ground state being probed. Thus the rotation is decreased with respect to the equilibrium case. The opposite is true for the blue-detuned beam. The m_F anisotropy is due to the pump polarization changing from its initially linear state to being highly elliptical as it propagates through the medium.

By taking the difference of the curves in Fig. 6, we can obtain the rotation caused by switching among the three cases of no control field and red- and blue-detuned control. Curves *A* and *B* in Fig. 7(i) show the magnitude of the rotation between the cases of control field on and off, with $\pi/2$ rotation and ~90% transmission for red detuning. Note that the red- and blue-detuned cases have opposite signs, so that the difference between these two (curve *C*) has a greater magnitude, achieving $\pi/2$ at ~95% transmission. The transmission from Fig. 7(ii) was used to calculate the optical density, which in turn was used to calculate the figure of merit, shown in Fig. 7(iii). The figure of merit is $>40\pi$ for probe detunings up to $5\Delta\omega_D$. This is more than an order of magnitude larger than in previous work; for example, it was 1.4π in Ref. [23] and $\pi \times 10^{-2}$ to $\pi \times 10^{-1}$ for other experiments [28–30]. From the theory curve, the figure of merit is essentially constant beyond two Doppler widths from resonance. This is ideal for broadband light, where large differential dispersion over the spectrum of the pulse can lead to distortion [16]. The theoretical and measured figures of merit do not agree close to zero detuning, since the probe beam was sufficiently strong to optically pump the medium and alter its own transmission through the medium; whereas the theory curve is based on the weak-probe limit, which in the case of the Rb D_1 line is 10 nW [31].

VII. CONCLUSION

In summary, we have demonstrated the controlled polarization rotation of one optical field due to the presence of another, with high transmission of both beams. A continuous-wave field was used to incoherently pump atoms into a dark ground state, a process that typically takes 0.1–1 μs [32]. Hence this process allows rapid switching and has applications as a dynamic half-wave plate, and as a tunable Faraday dichroic beam splitter [24].

In the current experiment, a relatively strong control field is required. In future work, a pulsed field will be used to coherently drive population into the excited state in a time less than the excited-state lifetime. A simulation of population dynamics shows that only a small amount of anisotropy in the occupation of atomic states is required to observe the rotations necessary to realize orthogonally polarized light channels. The nanosecond switching time combined with the gigahertz bandwidth off-resonant Faraday effect [16] could permit rapid high-fidelity switching at low light levels.

ACKNOWLEDGMENTS

This work is supported by EPSRC. We thank J. Millen and M. P. A. Jones for discussion, technical assistance, and the loan of equipment.

[1] B. Dayan and Y. Silberberg, Nature Photon. **3**, 429 (2009).
[2] I. Glesk, B. C. Wang, L. Xu, V. Baby, and P. R. Prucnal, Prog. Opt. **45**, 53 (2003).
[3] S. E. Harris and Y. Yamamoto, Phys. Rev. Lett. **81**, 3611 (1998).
[4] M. Yan, E. G. Rickey, and Y. Zhu, Phys. Rev. A **64**, 041801(R) (2001).
[5] M. O. Scully, Phys. Rev. Lett. **67**, 1855 (1991).
[6] M. O. Scully and M. Fleischhauer, Phys. Rev. Lett. **69**, 1360 (1992).
[7] N. A. Proite, B. E. Unks, J. T. Green, and D. D. Yavuz, Phys. Rev. Lett. **101**, 147401 (2008).
[8] D. Bouwmeester, A. K. Ekert, and A. Zeilinger, *The Physics of Quantum Information* (Springer, Berlin, 2000).
[9] J. Zhang, G. Hernandez, and Y. Zhu, Opt. Lett. **32**, 1317 (2007).
[10] A. M. C. Dawes, L. Illing, S. M. Clark, and D. J. Gauthier, Science **308**, 672 (2005).
[11] A. M. C. Dawes, L. Illing, J. A. Greenberg, and D. J. Gauthier, Phys. Rev. A **77**, 013833 (2008).
[12] R. G. Hunsperger, *Integrated Optics: Theory and Technology*, 5th ed. (Springer, Berlin, 2002).
[13] P. Siddons, C. S. Adams, and I. G. Hughes, J. Phys. B **42**, 175004 (2009).
[14] D. Budker *et al.*, Rev. Mod. Phys. **74**, 1153 (2002).
[15] J. Menders, K. Benson, S. H. Bloom, C. S. Liu, and E. Korevaar, Opt. Lett. **16**, 846 (1991).
[16] P. Siddons, N. C. Bell, Y. Cai, C. S. Adams, and I. G. Hughes, Nature Photon. **3**, 225 (2009).
[17] Z. K. Lee *et al.*, Appl. Phys. Lett. **69**, 3731 (1996).
[18] W. Happer and B. S. Mather, Phys. Rev. Lett. **18**, 577 (1967).
[19] W. F. Buell and M. Fink, Appl. Phys. B **60**, S227 (1995).
[20] C. Wieman and T. W. Hansch, Phys. Rev. Lett. **36**, 1170 (1976).
[21] K. Hammerer, A. S. Sorensen, and E. S. Polzik, Rev. Mod. Phys. **82**, 1041 (2010).
[22] M. Kubasik, M. Koschorrek, M. Napolitano, S. R. deEchaniz, H. Crepaz, J. Eschner, E. S. Polzik, and M. W. Mitchell, Phys. Rev. A **79**, 043815 (2009).
[23] S. Li, B. Wang, X. Yang, Y. Han, H. Wang, M. Xiao, and K. C. Peng, Phys. Rev. A **74**, 033821 (2006).
[24] R. P. Abel, U. Krohn, P. Siddons, I. G. Hughes, and C. S. Adams, Opt. Lett. **34**, 3071 (2009).
[25] H. Chen, C. Y. She, P. Searcy, and E. Korevaar, Opt. Lett. **18**, 1019 (1993).
[26] S. Huard, *Polarization of Light* (Wiley, New York, 1997).

[27] D. J. McCarron, I. G. Hughes, P. Tierney, and S. L. Cornish, Rev. Sci. Instrum. **78**, 093106 (2007).
[28] V. M. Entin, I. I. Ryabtsev, A. E. Boguslavsky, and Yu. V. Brzhazovsky, Opt. Commun. **207**, 201 (2002).
[29] J. M. Choi, J. M. Kim, and D. Cho, Phys. Rev. A **76**, 053802 (2007).
[30] X. Yang, S. Li, X. Cao, and H. Wang, J. Phys. B **41**, 085403 (2008).
[31] P. Siddons, C. S. Adams, C. Ge, and I. G. Hughes, J. Phys. B **41**, 155004 (2008).
[32] C. P. Pearman *et al.*, J. Phys. B **35**, 5141 (2002).